Protoplasma
https://doi.org/10.1007/s00709-026-02203-z

RESEARCH

Photoprotective strategies of *Haematococcus lacustris* in response to desiccation stress

Thomas Roach[1] · **Ginga Shimakawa**[2]

Received: 9 January 2026 / Accepted: 22 April 2026

Abstract

Water loss is a major challenge for photosynthetic organisms. Most are prone to drought stress and only few can tolerate full desiccation. Here, we investigated regulation of photosynthetic electron flow during dehydration and rehydration in *Haematococcus lacustris*, a desiccation tolerant green alga. During dehydration, non-photochemical quenching (NPQ) increased for dissipating excess light energy, while light-use efficiency of photosystems II (PSII) and I (PSI) decreased. The reaction centre of PSI (P700) became electron-limited at its donor side, helping form photoprotective $P700^+$. Inhibiting alternative oxidases with octyl gallate delayed chlorophyll fluorescence quenching, indicating that plastid terminal oxidases (PTOX) supported formation of NPQ during desiccation. Reduction rates of $P700^+$ during a saturating pulse were slower if cells dehydrated slower, showing that photoprotection was upregulated during desiccation acclimation. During rehydration, octyl gallate and diphenyleneiodonium (DPI), a flavoenzyme inhibitor, slowed oxidation of P700 under actinic light, indicating PTOX and flavodiiron proteins (FLV) were involved in maintaining $P700^+$. A similar response occurred with the protonophore nigericin. We conclude that beyond preventing over-reduction of the electron transport chain, PTOX and FLV facilitated thylakoid luminal acidification under low water stress, protecting photosystems via NPQ, photosynthetic control and $P700^+$ formation.

Keywords Photosynthesis · Desiccation · Alternative electron pathway · Drought · *Haematococcus pluvialis*

Introduction

Regulation of light harvesting efficiency, electron transport and transfer processes are indispensable for photosynthesis. It enables efficient carbon assimilation across a broad range of light intensities and under environmental challenges encountered in nature. At times, light energy is absorbed in excess of what is required, such as under stressful conditions that limit carbon assimilation. For example, dehydration and eventual desiccation impairs enzyme activity and thus photosynthesis. Without regulation, unwanted photochemistry and charge separation in still functional reaction centres otherwise produce reactive oxygen species (ROS) and cause damage (Roach and Krieger-Liszkay 2019; Challabathula et al. 2018). Imbalances between rates of photosynthetic electron flux and CO_2 assimilation is partially regulated by acidification of the thylakoid lumen. The pH of the lumen decreases with light intensity due to elevated PSII activity and proton-coupled electron flow in the cytochrome b_6f complex (cyt b_6f), both which release protons into the thylakoid lumen. Furthermore, cyclic electron flow uses stromal reducing power to re-reduce plastoquinone, promoting proton transfer via cyt b_6f (Fig. 1). As the pH of the lumen decreases, the plastoquinol oxidation step of the cyt b_6f slows, limiting electron flux to plastocyanin and photosystem I (PSI) in a process termed photosynthetic control. This protects PSI from over-reduction, as well as promoting oxidation of the PSI reaction centre (P700) (Klughammer and Schreiber 1994), that may protect PSI from photoinhibition (Shimakawa and Miyake 2018). Formation of photoprotective $P700^+$ under high light is also achieved with alternative PSI electron acceptors,

Handling Editor: Andreas Holzinger

✉ Thomas Roach
thomas.roach@uibk.ac.at

[1] Department of Botany, University of Innsbruck, Sternwartestraße 15, Innsbruck, Austria

[2] Graduate School of Agricultural Science, Kobe University, 1-1 Rokkodai-cho, Nada- ku, Kobe 657-8501, Hyogo, Japan

Published online: 04 May 2026

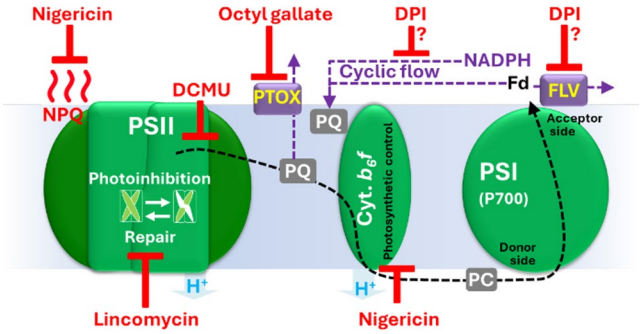

Fig. 1 A cross section of a thylakoid membrane showing the site of inhibitors used in this study. Green shapes show protein complexes involved in the photosynthetic electron transfer/transport chain and purple boxes show proteins involved in alternative electron pathways. Inhibitors are in red. Nigericin is a protonophore inhibiting the increase of proton gradient across thylakoid membrane, finally affecting NPQ and photosynthetic control. Arrows denote electron pathways. Cyt. b_6f: Cytochrome b_6f, DCMU: 3-(3,4-dichlorophenyl)−1,1-dimethylurea, DPI: Diphenyleneiodonium, Fd: Ferredoxin, FLV: flavodiiron, NPQ: Non-photochemical quenching, P700; PSI reaction centre chlorophyll, PC: Plastocyanin, PQ: Plastoquinone pool, PSII/I: Photosystem II/I, PTOX: plastid terminal oxidase

which in algae include flavodiiron (FLV) proteins that use stromal reductants to reduce O_2 to H_2O, thereby acting as an electron safety valve (Ilík et al. 2017). In the absence of FLV, a lower steady-state of $P700^+$ is formed and ROS production from partial reduction of O_2 increases (Pfleger et al. 2024). Furthermore, chlororespiration can also release excess reducing power, whereby NAD(P)H is used by a dehydrogenase to reduce the photosynthetic plastoquinone (PQ) pool. In algae, NDA2, a NADPH dehydrogenase of the PQ pool, is involved in chlororespiration (Jans et al. 2008). Subsequently, a plastid terminal oxidase (PTOX) oxidises plastoquinol, transferring electrons to O_2 and avoiding reduction of cyt b_6f (Houille-Vernes et al. 2011). Two genes for PTOX can be found in green algae (*PTOX1* and *PTOX2*), both which are conserved in the genome of *H. lacustris* and highly expressed under high light conditions (Wang et al. 2009). PTOX1 has been attributed to carotenoid synthesis (Wang et al. 2009), including astaxanthin that is rapidly accumulated under high light, or in response to desiccation (Roach et al. 2022a), while in *C. reinhardtii* PTOX2 has been confirmed to function in chlororespiration (Houille-Vernes et al. 2011). In the model chlorophyte *Chlamydomonas reinhardtii*, PTOX2 and FLV have been shown as important safety valves of photosynthetic electron flow under stressful conditions, such as light fluctuations (Nawrocki et al. 2019; Chaux et al. 2017). However, if FLV and PTOX regulate electron flow during desiccation/rehydration is not known.

During dehydration, quantum yields of photosystems decrease, and thus also the threshold when light becomes excess. This requires regulation of light harvesting to modulate photosystem activities, such as via high-energy-state quenching (qE)-type non-photochemical quenching (NPQ), comprising in green algae of zeaxanthin accumulation via the xanthophyll cycle and protonation of LHCSR proteins that protect both photosystems (Erickson et al. 2015; Roach et al. 2020; Beckett et al. 2021). qE-type NPQ facilitates a safe dissipation of light energy to heat in the antenna before it reaches the photosystem reaction centres. Some regulatory mechanisms employed by desiccation-tolerant organisms during dehydration are the same as those that occur under high/excess light. For example, a light-independent desiccation-induced accumulation of zeaxanthin occurs in vascular and non-vascular plants (Fernández-Marín et al. 2021). Even with qE-type NPQ active, both PSI and PSII contain reaction centre chlorophylls that if excited could initiate photochemistry. However, in the desiccated state, light energy absorbed by photosystems is dissipated rather than converted into electrochemical energy. Evidence in cyanobacteria, moss and algal lichen photobionts showed the quencher to be PS reaction centre chlorophyll cations, either in PSII ($P680^+$) or PSI ($P700^+$) (Bar-Eyal et al. 2015; Heber et al. 2011; Yamakawa et al. 2012; Slavov et al. 2013). This again highlights the importance of maintaining $P700^+$ under stressful conditions.

Haematococcus lacustris, previously known as *H. pluvialis*, can survive full desiccation, and similar to other desiccation-tolerant algae (e.g. lichen photobionts) down-regulates photosynthesis, but maintains its photosynthetic apparatus (Roach et al. 2022a; Holzinger and Karsten 2013; Kranner et al. 2005). Flagellate *H. lacustris* macrozooids are not constitutively desiccation tolerant, as tested by rapid dehydration. Inducing desiccation tolerance in flagellate macrozooids took ~ 3 days of acclimation via atmospheric exposure, while keeping cells hydrated, in a process requiring photosynthesis and coinciding with astaxanthin-rich lipid accumulation (Roach et al. 2022a). During this process, cells changed to green palmella that turned deep red due to astaxanthin accumulation. Post desiccation, the same cells could resume photosynthetic activity within hours of rehydration (Roach et al. 2022a). Formation of red palmella is a typical response of this species to environments unfavourable for growth, whereby cells develop into nonmotile palmella, which are constitutively desiccation tolerant (Vávrová et al. 2024). If stress conditions prevail, palmella transform into haematocyst aplanospores.

In summary, achieving desiccation tolerance in *H. lacustris* requires photosynthesis, but photosynthetic electron pathways also require regulation to prevent excessive ROS production during the stresses imposed by low water availability. How this is achieved is unclear. On the one hand, alternative electron pathways, such as FLV and PTOX, may act as safety valves of an over-reduced electron transfer/transport chain, while on the other they can support luminal

acidification by enabling electron flow if $NADP^+$ availability is restricted. Luminal acidification is central to qE-type NPQ, photosynthetic control and thus $P700^+$ formation. We therefore hypothesised that these alternative electron pathways are important in the desiccation tolerance of *H. lacustris* and become upregulated during acclimation. To test this, we measured PSII and PSI in desiccation-acclimated and non-acclimated cells, and made use of alternative electron pathway inhibitors (Fig. 1) during dehydration and rehydration.

Methods

Growth, desiccation and rehydration

Haematococcus lacustris was purchased as *H. pluvialis* strain 34-1b from the Sammlung von Algenkulturen (SAG; University of Göttingen). Growth of photoautotrophic liquid cultures, containing mostly macrozooids and occasional green palmella, was in sterile-air-bubbled Bold's Basal Medium that contained three-fold more nitrogen than standard (3 N-BBM), under continuous illumination at 50 µmol photons m^{-2} s^{-1}, at 20–23 °C, according to Roach et al. (2022a). For desiccation and rehydration treatments, cells in 2 mL of liquid culture during the exponential growth phase were filtered with vacuum pump onto 25-mm cellulose-acetate filters with 5 µm pore size (Satorius). For desiccation acclimation, whereby all cells transition to red palmella and possibly some haematocysts, cellulose-acetate filters with the cells were placed onto two 85-mm cellulose Whatman no. 1 filter papers in a crystal polystyrene Petri dish saturated with 3 mL of de-ionized H_2O. For rapid desiccation, cells were placed onto dry Whatman filter papers. The lids of Petri dishes were replaced and left unsealed and put under the same conditions as used for culture growth. The relative humidity (RH) was between 46 and 47%. Water contents were measured by the difference between fresh and dry weights of cells and filter together. For rehydration, cells on filters were saturated with de-ionized water (+/- inhibitors, see below) and placed under growth conditions.

Inhibitor treatments

Cells were treated at with 10 µM 3-(3,4-dichlorophenyl)−1,1-dimethylurea (DCMU), 10 µM nigericin hydrochloride salt, 10 µM diphenyleneiodonium (DPI), or 10 µM octyl gallate, from a 10 mM stock solution in methanol. For investigating influences during desiccation, inhibitors were added to liquid cultures 5 min before transfer to cellulose-acetate filters and immediate rapid desiccation, as above without acclimation. For investigating the influence of inhibitors during rehydration, desiccation-acclimated cells were rehydrated from the desiccated state on filters in de-ionized water containing the inhibitors prepared, as above, under the same conditions used for culture growth. Lincomycin hydrochloride salt was dissolved in de-ionized water at a concentration of 2.5 mM for direct use.

Chlorophyll fluorescence and $P700^+$ absorbance analyses

Measurements of chlorophyll fluorescence were either made using a Maxi Imaging PAM (Walz), or in combination with redox changes of PSI reaction centre chlorophyll (P700) using a DUAL-PAM 100 (Walz). The maximum (F_v/F_m) and relative (Y[II]) quantum yields of PSII were calculated via $\frac{Fm-Fo}{Fm}$ and $\frac{Fm-Ft}{Fm}$, respectively, with F_o and F_t referring to pre saturating pulse fluorescence yields in the dark and under actinic light, respectively. F_m was measured with a 300 ms saturating pulse of 3000 µmol photons m^{-2} s^{-1}. For measuring F_v/F_m a dark adaption of 30 min was given before measurement and for Y[II], measurements were made after 2 min pre-treatment at near growth light intensity (53 µmol photons m^{-2} sec^{-1}) to activate carbon assimilation and then after 2 min under 95 µmol photons m^{-2} s^{-1}. The quantum yield of NPQ (Y[NPQ]) of rapidly desiccating cells was calculated via $\left(\frac{Fo}{Fm}\right) - \left(\frac{Fo}{Fm}\right)$, whereby F_m' corresponds to F_m during desiccation. The experiment was performed under 10 µmol photons m^{-2} sec^{-1}.

For DUAL-PAM measurements, cells on cellulose-acetate filter were placed in a transparent film between the light source and detectors, enabling absorbance measurements of $P700^+$. To measure maximum and minimum $P700^+$ values (P_m and P_o, respectively), cells were treated with 5 s of maximum intensity far-red light followed by a ~800 ms saturating pulse. The P_m was measured as maximum signal (i.e. between 5–10 ms during the saturating pulse) and P_o 550 ms after the saturating pulse had finished. The P700 and fluorescence measuring light intensities were set to 10. For calculating all $P700^+$ reduction rates, data was exported and adjusted to P_m=1 and P_o=0 on an individual measurement basis. Time spans used for calculating reduction rates were decided in accordance with fastest $P700^+$ kinetic changes and are reported in Figure legends. There is an apparent increase in signal immediately after the pulse finishes, which we consider noise and disregarded for calculation of P_m and $P700^+$ reduction. Measurements during desiccation acclimation were made after 2 min pre-treatment at near growth light intensity (53 µmol photons m^{-2} sec^{-1}) followed by 2 min actinic light of 95 µmol photons m^{-2} sec^{-1} using the same saturating pulse as for measuring P_m, but without far-red light pre-treatment. Donor side limitation (Y[ND]) of P700 was calculated by the $P700^+$ value before

a saturating pulse ($P700_{ox}$) without far-red illumination as $\frac{P700ox}{Pm}$. Quantum yields of PSI (Y[I]) were calculated via $\frac{Pm'-P700ox}{Pm}$ whereby P_m' corresponds to P_m in actinic light (Klughammer and Schreiber 1994). All raw data of P700 kinetics can be found in Table S1.

Oxygen flux

The influence of octyl gallate on oxygen flux was measured using a Fibox 3 optode dipping probe (PreSens) in 2 mL of liquid culture with constant stirring at 25 °C. Oxygen consumption was measured before (respiration) and at 250 µmol photons m^{-2} s^{-1} (photosynthesis).

HPLC quantification of photosynthetic pigments

Cells were ground on the cellulose-acetate filter in a 2 mL reaction tube with two 5-mm quartz beads. One filter containing cells was used for each replicate. The samples were cooled to −80 °C before grinding for 1 min at a frequency of 30 Hz in a Tissuelyser II (Qiagen). Pigments were extracted by addition of 400 µL of methanol and shaken for 2 min at 30 Hz, before centrifugation at 26,000 *g* for 40 min at 4 °C. For analysis, 20 µL was injected into an Agilent 1100 HPLC system equipped with a LiChrospher 100 RP-18 (125 × 4 mm, 5 µm) column, according to (Roach et al. 2022a), and amounts of violaxanthin (V), antheraxanthin (A) and zeaxanthin (Z) were calculated using pure standards. The xanthophyll de-epoxidation ratio was calculated as %, according to $\frac{0.5A+Z}{(V+A+Z)} * 100$.

Statistics

Statistical comparisons were conducted in OriginPro 2025. Significant differences between groups were determined using one-way ANOVA and subsequent Tukey *post hoc* test with significance value of 0.05. Alternatively, when comparisons were only made to control, a one-way *t*-test assuming unequal sample variance was performed with $p < 0.01$ or $p < 0.001$, as indicated in Figure legends.

Results

We first measured the response of photosynthesis during acclimation to desiccation. Cells from liquid cultures were filtered onto cellulose-acetate papers for atmospheric exposure in the light, while maintaining hydration from below with damp filter paper. Maximum PSII quantum yields (F_v/F_m), and relative quantum yields of PSII (Y[II]) and PSI (Y[I]) under light, decreased with increasing acclimation time (Fig. 2a-c). As the filter paper started to dry out by 7 d, Y[II] and Y[I] decreased further, until desiccation was reached on day eight and both dropped to near zero. Values of F_v/F_m and the maximum level of $P700^+$ (P_m) had a positive relationship with water content (Fig. S1), both declining as cells dehydrated.

Near-infrared absorbance changes of PSI reaction centre chlorophyll (P700) showed that lowered electron flow through PSI during desiccation acclimation and dehydration was due to increased donor-side limitation (Y[ND]), e.g. electron availability (Fig. 2d). In contrast, acceptor-side limitation (Y[NA]) declined between 3 and 8 days (Fig. S2). The $P700_{ox}$, i.e. how oxidised P700 is before a saturating pulse, is reflective of how reduced the electron transport chain is. Since DCMU blocks electron transport out of PSII (linear flow), but $P700_{ox}$ was not at P_m, cyclic electron flow could have been keeping P700 from fully oxidising (Fig. 3a). Dehydrating cells also had a higher $P700_{ox}$ than hydrated control (Fig. 3a). P_m is rapidly reached within a few milliseconds during a saturating light pulse. Soon after, electrons released by PSII reach PSI and reduce P700 (decrease in $P700^+$ signal) that can be abolished by the PSII inhibitor DCMU (Fig. 3a). Subsequently, electrons are accepted from PSI (e.g. via FLV) faster than they enter leading to a re-oxidation of P700 (Ilík et al. 2017), here seen from 200 ms. An acidic lumen could also slow electrons entering PSI via photosynthetic control. Darkness inhibits excitation of P700 and electron transfer out of PSI, thus the rate of $P700^+$ loss post saturating pulse is combination of the number of available upstream electrons, including from cyclic electron flow, and photosynthetic control. DCMU lowered P700 reduction rates five-fold in the dark post-saturating pulse (Fig. S3), indicating ~20% of electron flow was cyclic.

Rates of $P700^+$ reduction slowed during dehydration, both during (in light) and immediately (in darkness) after a saturating pulse (Fig. 3b), indicating a relation between both rates. During rapid desiccation without acclimation, rates of $P700^+$ reduction in the dark relative to reduction rates in the light were lower than with acclimation (Fig. 3b), showing acclimation-affected electron pathways or photosynthetic control. Three data points of late rehydrated desiccation-acclimated cells align with non-acclimated cells (Fig. 3b), indicating they returned to a non-acclimated state.

To explore regulators of electron flow, we used inhibitors of alternative oxidases, such as PTOX, with octyl gallate. Steady state chlorophyll fluorescence levels (F_t) of non-light-stressed cells are informative of the redox state of the PQ pool. In hydrated cells kept in the dark, 10 µM octyl gallate increased F_t without loss of F_m, indicating PTOX was helping keep the PQ pool oxidised as part of chlororespiration (Fig. S4), in agreement with the measured cyclic electron flow (Fig. 3a). Octyl gallate inhibits both chloroplast

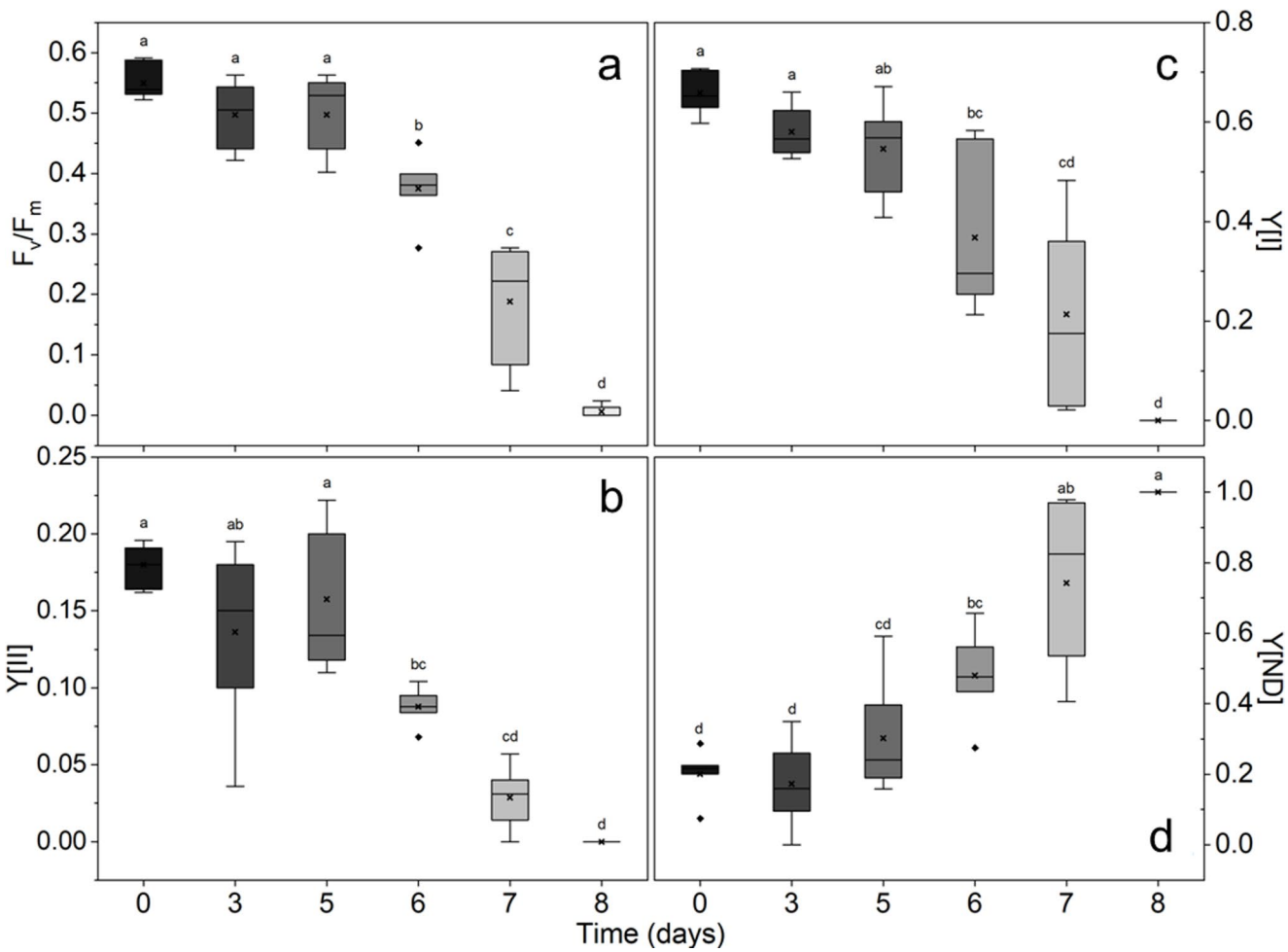

Fig. 2 Down-regulation of photosynthesis during acclimation to desiccation and actual dehydration. Cells were filtered onto cellulose-acetate papers for atmospheric exposure, while maintaining hydration from below with damp filter paper, which dried between 6–8 days. Box plots show **(a)** maximum (F_v/F_m), and **(b)** relative (Y[II]) quantum yields of photosystem II, **(c)** relative quantum yields of photosystem I (Y[I]) and **(d)** donor side limitation on photosystem I yields (Y[ND]). Box lengths are 25–75% of values, with whiskers of min-max values on a scale between 0–1 for all parameters. Y[II], Y[I] and Y[ND] were measured after 2 min at 95 µmol photons m^{-2} s^{-1} following activation of carbon assimilation for 2 min at growth light intensity. Different letters indicate significant differences at $p < 0.05$, according to a Tukey *post-hoc* test, $n = 5–6$

(PTOX) and mitochondrial alternative oxidases (AOX). At growth light intensity, 10 µM octyl gallate lowered net oxygen production by 42%, while in the dark net oxygen consumption was 13% lower, compared to control (Fig. S4), indicating PTOX had more of an influence on photosynthesis than AOX had on respiration. Under high light, 10 µM octyl gallate also lowered NPQ values (Fig. S5), indicating a contribution of PTOX to formation of a trans-thylakoid ΔpH. Nigericin also impaired light-activated NPQ, confirming the involvement of a ΔpH (Fig. S5). Moreover, octyl gallate delayed onset of NPQ during rapid desiccation to a similar extent as occurred in the presence of nigericin (Fig. 4). We also used diphenyleneiodonium (DPI), an inhibitor of flavin-containing enzymes, which also significantly delayed onset of NPQ, but to a lesser extent than octyl gallate (Fig. 4). Overall, the results suggest that PTOX and a flavin-enzyme were involved in the desiccation-induced formation of a trans-thylakoid ΔpH.

Octyl gallate and DPI had limited effect on Y(ND) or $P700^+$ reduction rates during a saturating pulse (Fig. S3). However, octyl gallate increased the dark reduction rate of $P700^+$ post saturating pulse, whereas DPI slowed it (Fig. S3). Considering all inhibitor treatments during dehydration, maximum $P700^+$ reduction rates in the light and Y(ND) negatively correlated ($R^2 = 0.77$) (Fig. S3), possibly by an involvement of a ΔpH via photosynthetic control in both processes.

To explore mechanism of PSII down-regulation during desiccation acclimation (e.g. lowered F_v/F_m as in Fig. 2a), we measured xanthophyll concentrations, damage to PSII and chlorophyll fluorescence kinetics during rehydration. Actinic light had a very limited influence on chlorophyll

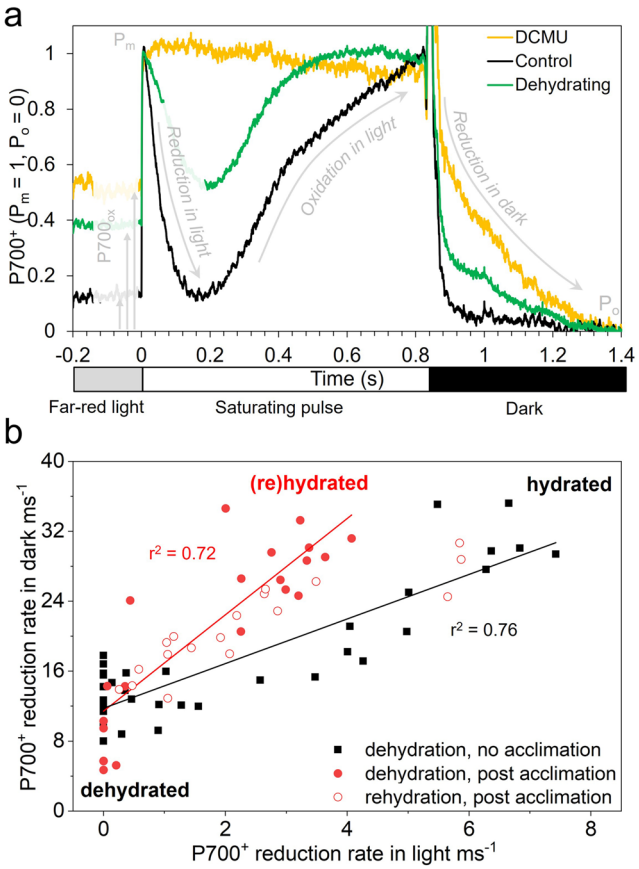

Fig. 3 Effects of dehydration and rehydration on redox changes of photosystem I reaction centre (P700). **(a)** Typical P700 redox kinetics with values shown relative to maximum $P700^+$ (P_m) = 1 and minimum (P_o) = 0. Black is hydrated control, yellow is hydrated with 10 µM 3-(3,4-dichlorophenyl)−1,1-dimethylurea (DCMU) and green is late in desiccation acclimation. $P700_{ox}$ is the redox state pre saturating pulse after treatment with far-red light for 5 s. The saturating light pulse started at 0 ms, reaching P_m at ~10 ms, after which a light-induced reduction of $P700^+$ occurs (10–200 ms), and subsequently recovery of oxidation of P700 (200–850 ms), and then its re-reduction in darkness. **(b)** Correlation of PSI reduction rates early during the saturating pulse ('light'; 50–150 ms) and post saturating pulse ('dark'; 860–875 ms), as measured in (a). Cells were desiccated with (red circles) or without (black squares) desiccation acclimation and measured during dehydration (filled symbols) or rehydration (open symbols). Each symbol is of an individual measurement. Lines of best fit are of dehydrating samples only

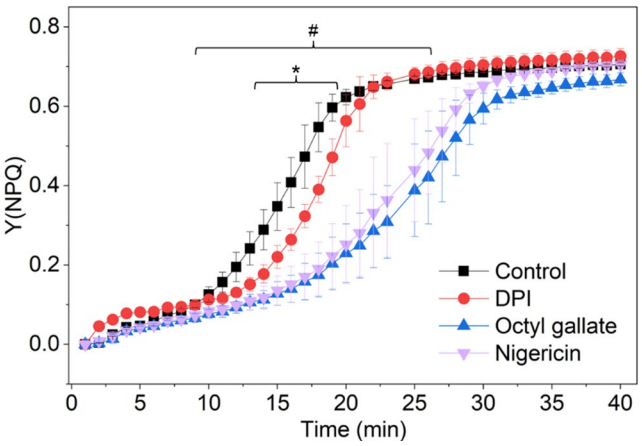

Fig. 4 Effects of electron transport inhibitors and the uncoupler nigericin on yields of non-photochemical quenching (Y[NPQ]) during rapid desiccation. Cells were treated with 10 µM of either nigericin, octyl gallate or diphenyleneiodonium (DPI) for 5 min before initiating desiccation. Symbols are means ± SD, with Y[NPQ] on a scale between 0–1. Brackets labelled with a hash and asterisk indicate significantly different time-spans at $p < 0.01$ relative to control for octyl gallate and DPI, respectively, according to a *t*-test, $n = 4$

fluorescence in desiccated cells, which even in the dark was completely quenched (Fig. 5a). After 2.5 h rehydration, some quenching had relaxed, but there was very little photochemical quenching or NPQ detectable in response to actinic light, indicating the PQ pool was highly reduced, perhaps due to photosynthetic control. After 24 h rehydration, F_v/F_m values were similar to pre-desiccation (Fig. 5b) and cells had recovered high-light inducible NPQ (Fig. 5a). A high level of zeaxanthin was found in desiccated cells that decreased during rehydration, alongside accumulation of violaxanthin, lowering the de-epoxidation ratio of xanthophyll cycle as cells recovered from desiccation (Fig. 5c). PSII also had become damaged by desiccation, as shown by rehydration in the presence of lincomycin that prevents PSII repair. In the presence of lincomycin, F_v/F_m after 24 h rehydration was > 3-fold lower than in its absence (Fig. 5b). During rehydration, ca. 50% of P_m was restored within 15 min, much faster than recovery of F_v/F_m (Fig. S6), and within a few hours was fully restored, indicating that PSI was not critically damaged by desiccation, and that the P_m decrease as cells dehydrated (Fig. S1) was due to other reasons (e.g. cell shrinkage).

During rehydration, nigericin nearly doubled the light-induced rate of PSI reduction during a saturating pulse, while octyl gallate and DPI slightly increased reduction rates, resulting in P_m not being reached in the later phase of the saturating pulse (Fig. 6a). The effect of inhibitors was also prominent in response to actinic light, whereby it took 3 s in control cells to reach P_m at 200 µmol photons $m^{-2}s^{-1}$, but ≥10 s in the presence of octyl gallate or DPI, while nigericin completely prevented oxidation of P700 (Fig. 6b). The same trend, but to a lesser extent, was observed when cells were treated with far-red light (Fig. 6c), indicating the response was enhanced by PSII activity. Thus, relieving photosynthetic control at cyt b_6f (nigericin), or inhibiting PTOX (octyl gallate), slowed the accumulation of $P700^+$ under actinic light. Notably, DPI had an almost identical influence on $P700^+$ kinetics as compared to octyl gallate (Fig. 6). To further show the activity of chlororespiration, chlorophyll fluorescence kinetics were followed in rehydrated cells (Fig. S7) in a protocol developed for algae by Roach (2022). In the dark post high-light treatment, the drop in F_m is attributed to

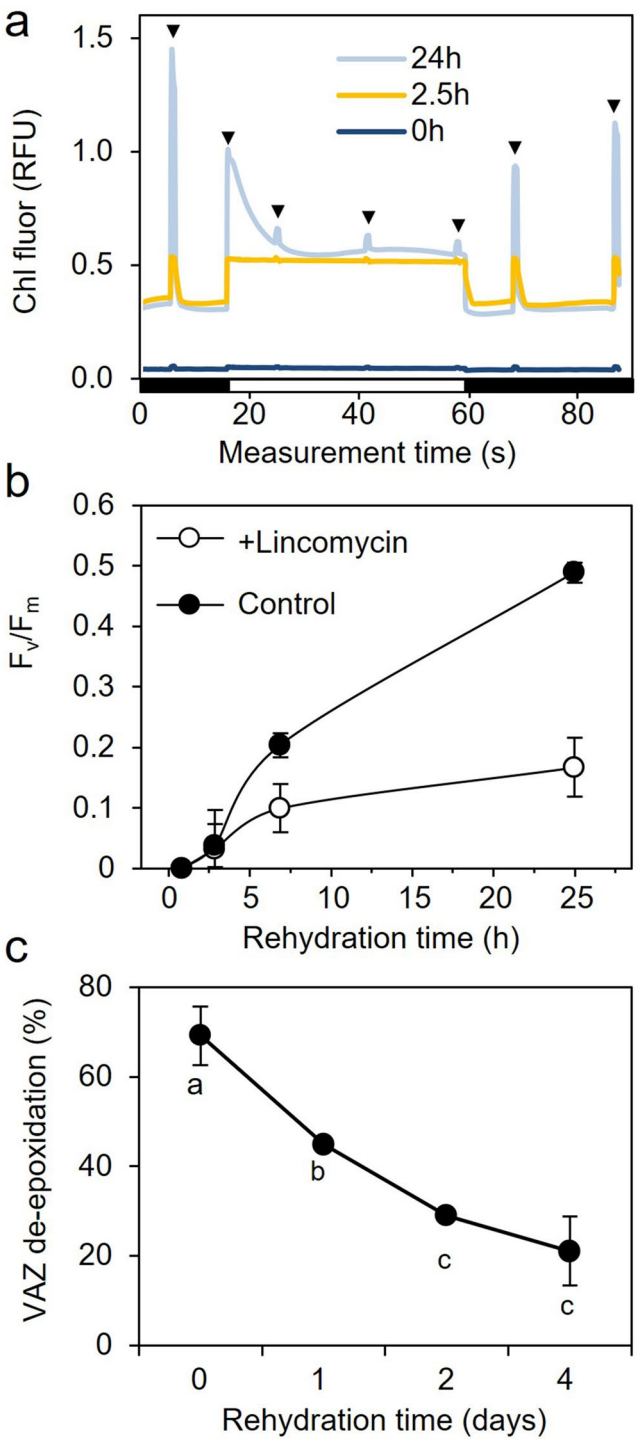

Fig. 5 Recovery of desiccation-induced down regulation of photosystem II during rehydration of desiccation-acclimated cells. **(a)** Typical chlorophyll fluorescence (Chl fluo) quenching kinetics of cells 0, 2.5 and 24 h after initiating rehydration. Saturating pulses are indicated by arrow heads and dark and light during the quenching kinetic are indicated by black and white bars below the x-axis. **(b)** Recovery of maximum quantum yields of photosystem II (F_v/F_m) during rehydration of control (black) and lincomycin-treated (white) cells, $n = 3 \pm$ SD. **(c)** Rehydration induced changes in violaxanthin (V), antheraxanthin (A) and zeaxanthin (Z) contents, as expressed as the VAZ de-epoxidation ratio during rehydration. Cells were harvested from growth light. Different letters in (**c**) indicate significant differences across time at $p < 0.05$ according to a Tukey *post-hoc* test, $n = 3$

transition to state 2 (phosphorylated LHCII decoupled from PSII) due to reduction of the PQ pool (chlororespiration), as demonstrated with LHCII phosphorylation in *C. reinhardtii* (Roach and Na 2017). Transition can be reversed to state 1 (dephosphorylated LHCII coupled to PSII) by far-red light that stimulates PSI more than PSII, oxidising the PQ pool and increasing F_m (Fig. S7).

Discussion

Previously, it was shown in *H. lacustris* that desiccation acclimation processes include lowering chlorophyll levels and increasing low-molecular-weight antioxidant defences (Roach et al. 2022a, b). Here, we focused on regulation of photosynthetic electron transport, which is important to maintain PSI from over-reduction under environmental fluctuations that limit carbon assimilation, and prevent critical levels of ROS production. Furthermore, oxidised PSI (i.e. $P700^+$) is an important energy dissipator in desiccated cells (Heber et al. 2011). Photoinhibition of PSI is a lethal event for photosynthetic organisms (Sonoike 2025), which is why a variety of molecular mechanisms function for P700 oxidation. Down regulation of photosynthesis requires careful coordination because some photosynthesis is required for desiccation intolerant *H. lacustris* cells in liquid culture to achieve desiccation tolerance (Roach et al. 2022a). We found that Y(ND) increased during desiccation acclimation (Fig. 2d) when cells gain desiccation tolerance while still hydrated, indicating this was a coordinated event. Indeed, $P700^+$ reduction rates also indicated that changes to electron flow had occurred upon acclimation (Fig. 3). Both F_v/F_m and Y(II) decreased during acclimation (Fig. 2a, b), indicating PSII photoinhibition was induced, as confirmed by lack of F_v/F_m recovery in cells rehydrated with lincomycin that prevents PSII repair (Fig. 5b). Nonetheless, F_v/F_m increased within hours of rehydration in control cells (Fig. 5b; Fig. S6), showing desiccation-induced PSII photoinhibition was not critical. Down-regulation of PSII involved activation of the xanthophyll cycle (Fig. 5c) that functions in qE-type NPQ.

An increasingly acidic thylakoid lumen during desiccation may have upregulated photosynthetic control to increase Y(ND). Since nigericin delayed onset of desiccation-induced NPQ (Fig. 4), we can be confident that the lumen was becoming more acidic during desiccation, with PTOX contributing to this process. Propyl gallate, a PTOX

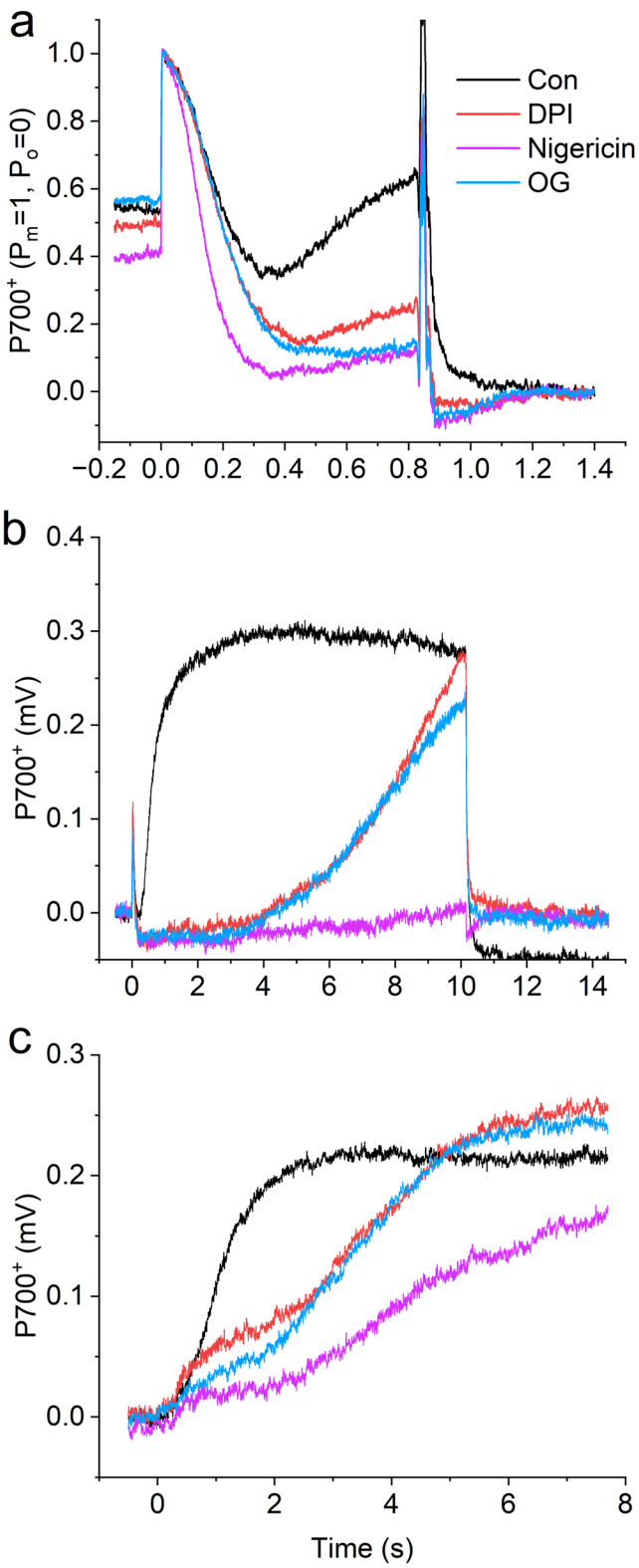

Fig. 6 Effects of the uncoupler nigericin and electron flow inhibitors on redox changes of photosystem I reaction centre chlorophyll (P700) after 3 h rehydration. Cells were treated with 10 µM of either nigericin (nig, violet), diphenyleneiodonium (DPI, red) or octyl gallate (OG, blue), or untreated (Con, black) before measurement. **(a)** $P700^+$ signals in response to a saturating light pulse, with values shown relative to maximum $P700^+$ (P_m) = 1 and minimum (P_o) = 0, as measured in Fig. 3a. The saturating pulse started at 0 s. $P700^+$ kinetics in response to **(b)** 202 µmol photons m^{-2} s^{-1} actinic light, and **(c)** far-red light of dark-adapted cells. Average kinetics of four independent measurements are shown

inhibitor similar to octyl gallate, promoted PSII photoinhibition under high light in *H. lacustris* (Zhao et al. 2021). In land plants, *PTOX* expression increases under drought stress (Ghotbi-Ravandi et al. 2019), and PTOX was shown to protect PSII (Calzadilla et al. 2024) and PSI (Messant et al. 2024) under high light stress. In the halophile *Eutrema salsugineum*, PTOX could account for up to 30% of total electron flux under salt stress (Stepien and Johnson 2009), while in *Ranunculus glacialis*, an alpine extremophile, PTOX was more abundant in sun compared to shade leaves, and was shown to act as a safety valve of the PQ pool (Laureau et al. 2013). Thus, building evidence suggests PTOX can play a role in diverse stress tolerances. While electron "safety valve" is an often-used term for the function of PTOX, it should not be forgotten that by enabling electron flow PTOX can help build a ΔpH from water-splitting by PSII and subsequent proton release into the lumen (Fig. 1). PTOX is widely conserved in photosynthetic eukaryotes, including plants, green algae, and most red and red-plastid secondary algae (Nawrocki et al. 2015; Messant et al. 2021). Several species across these groups of photosynthetic organisms live in environments exposed to desiccation (Holzinger and Karsten 2013). Alternative electron pathways have been described to contribute to stress tolerance in lichenized algae (Beckett et al. 2023), but we show here for the first time that PTOX helps promote photoprotection by building a ΔpH as part of the desiccation response.

During rehydration, DPI slowed accumulation of $P700^+$ (Fig. 6). Since in the latter stages of a saturating pulse $P700^+$ hardly formed in the presence of DPI (Fig. 6), as would be expected if FLV activity was fully functional (Ilík et al. 2017), it seems likely that either FLV, or FNR that supplies electrons to FLV, contributed. Early experiments also showed DPI affected PSI electron flow (Watling-Payne and Selwyn 1974), although as DPI is general flavoenzyme inhibitor, further research is required to substantiate a role for FLV in desiccation tolerance.

Supplementary Information The online version contains supplementary material available at https://doi.org/10.1007/s00709-026-02203-z.

Acknowledgements We acknowledge the insightful comments provided by the two anonymous reviewers.

Author contributions T.R. conceived the study, T.R. conducted the experiments and wrote the main manuscript text, G.S. helped with data analyses and interpretation. Both authors reviewed the manuscript.

Funding Open access funding provided by University of Innsbruck and Medical University of Innsbruck.

Data availability All data supporting the findings of this study are available within the paper and its Supplementary Information.

Declarations

Competing interests The authors declare no competing interests.

References

Bar-Eyal L, Eisenberg I, Faust A, Raanan H, Nevo R, Rappaport F, Krieger-Liszkay A, Sétif P, Thurotte A, Reich Z, Kaplan A, Ohad I, Paltiel Y, Keren N (2015) An easily reversible structural change underlies mechanisms enabling desert crust cyanobacteria to survive desiccation. Biochim Biophys Acta Bioenerg 1847(10):1267–1273. https://doi.org/10.1016/j.bbabio.2015.07.008

Beckett RP, Minibayeva F, Solhaug KA, Roach T (2021) Photoprotection in lichens: adaptations of photobionts to high light. Lichenologist 53(1):21–33. https://doi.org/10.1017/S0024282920000535

Beckett RP, Roach T, Minibayeva F, Werth S (2023) Alternative electron transport pathways contribute to tolerance to high light stress in lichenized algae. Physiol Plant 175(2):e13904. https://doi.org/10.1111/ppl.13904

Calzadilla PI, Song J, Gallois P, Johnson GN (2024) Proximity to photosystem II is necessary for activation of plastid terminal oxidase (PTOX) for photoprotection. Nat Commun 15:287. https://doi.org/10.1038/s41467-023-44454-x

Challabathula D, Zhang Q, Bartels D (2018) Protection of photosynthesis in desiccation-tolerant resurrection plants. J Plant Physiol 227:84–92. https://doi.org/10.1016/j.jplph.2018.05.002

Chaux F, Burlacot A, Mekhalfi M, Auroy P, Blangy S, Richaud P, Peltier G (2017) Flavodiiron proteins promote fast and transient O2 photoreduction in *Chlamydomonas*. Plant Physiol 174(3):1825–1836. https://doi.org/10.1104/pp.17.00421

Erickson E, Wakao S, Niyogi KK (2015) Light stress and photoprotection in *Chlamydomonas reinhardtii*. Plant J 82(3):449–465. https://doi.org/10.1111/tpj.12825

Fernández-Marín B, Roach T, Verhoeven A, García-Plazaola JI (2021) Shedding light on the dark side of xanthophyll cycles. New Phytol 230(4):1336–1344. https://doi.org/10.1111/nph.17191

Ghotbi-Ravandi AA, Shariati M, Shobbar Z-S, Shahbazi M (2019) Expression pattern and physiological roles of plastid terminal oxidase (PTOX) in wild and cultivated barley genotypes under drought stress. Environ Exp Bot 162:313–320. https://doi.org/10.1016/j.envexpbot.2019.03.007

Heber U, Soni V, Strasser RJ (2011) Photoprotection of reaction centers: thermal dissipation of absorbed light energy vs charge separation in lichens. Physiol Plant 142(1):65–78. https://doi.org/10.1111/j.1399-3054.2010.01417.x

Holzinger A, Karsten U (2013) Desiccation stress and tolerance in green algae: consequences for ultrastructure, physiological and molecular mechanisms. Front Plant Sci 4:327. https://doi.org/10.3389/fpls.2013.00327

Houille-Vernes L, Rappaport F, Wollman F-A, Alric J, Johnson X (2011) Plastid terminal oxidase 2 (PTOX2) is the major oxidase involved in chlororespiration in *Chlamydomonas*. Proc Natl Acad Sci U S A 108:20820–20825. https://doi.org/10.1073/pnas.1110518109

Ilík P, Pavlovič A, Kouřil R, Alboresi A, Morosinotto T, Allahverdiyeva Y, Aro EM, Yamamoto H, Shikanai T (2017) Alternative electron transport mediated by flavodiiron proteins is operational in organisms from cyanobacteria up to gymnosperms. New Phytol 214(3):967–972. https://doi.org/10.1111/nph.14536

Jans F, Mignolet E, Houyoux P-A, Cardol P, Ghysels B, Cuiné S, Cournac L, Peltier G, Remacle C, Franck F (2008) A type II NAD(P)H dehydrogenase mediates light-independent plastoquinone reduction in the chloroplast of *Chlamydomonas*. Proc Natl Acad Sci U S A 105:20546–20551. https://doi.org/10.1073/pnas.0806896105

Klughammer C, Schreiber U (1994) An improved method, using saturating light pulses, for the determination of photosystem I quantum yield via P700+-absorbance changes at 830 nm. Planta 192(2):261–268. https://doi.org/10.1007/BF00194461

Kranner I, Cram WJ, Zorn M, Wornik S, Yoshimura I, Stabentheiner E, Pfeifhofer HW (2005) Antioxidants and photoprotection in a lichen as compared with its isolated symbiotic partners. Proc Natl Acad Sci U S A 102(8):3141–3146. https://doi.org/10.1073/pnas.0407716102

Laureau C, de Paepe R, Latouche G, Moreno-Chacón M, Finazzi G, Kuntz M, Cornic G, Streb P (2013) PTOX in alpine plants. Plant Cell Environ 36:1296–1310. https://doi.org/10.1111/pce.12059

Messant M, Shimakawa G, Perreau F, Miyake C, Krieger-Liszkay A (2021) Evolutive differentiation between alga- and plant-type plastid terminal oxidase: study of plastid terminal oxidase PTOX isoforms in *Marchantia polymorpha*. Biochimica et Biophysica Acta (BBA) - Bioenergetics 1862(1):148309. https://doi.org/10.1016/j.bbabio.2020.148309

Messant M, Hani U, Lai TL, Wilson A, Shimakawa G, Krieger-Liszkay A (2024) Plastid terminal oxidase (PTOX) protects photosystem I and not photosystem II against photoinhibition in *Arabidopsis thaliana* and *Marchantia polymorpha*. Plant J 117(3):669–678. https://doi.org/10.1111/tpj.16520

Nawrocki WJ, Tourasse NJ, Taly A, Rappaport F, Wollman FA (2015) The plastid terminal oxidase: its elusive function points to multiple contributions to plastid physiology. Annu Rev Plant Biol 66:49–74. https://doi.org/10.1146/annurev-arplant-043014-114744

Nawrocki WJ, Buchert F, Joliot P, Rappaport F, Bailleul B, Wollman FA (2019) Chlororespiration controls growth under intermittent light. Plant Physiol 179(2):630–639. https://doi.org/10.1104/pp.18.01213

Pfleger A, Arc E, Grings M, Gnaiger E, Roach T (2024) Flavodiiron proteins prevent the Mehler reaction in *Chlamydomonas reinhardtii*. Biochimica et Biophysica Acta (BBA) - Bioenergetics 1865(4):149497. https://doi.org/10.1016/j.bbabio.2024.149497

Roach T (2022) Chlorophyll fluorescence of Chlamydomonas reinhardtii: insights into the complexities. Bioenerg Commun 10. https://doi.org/10.26124/bec:2022-0010

Roach T, Krieger-Liszkay A (2019) Photosynthetic regulatory mechanisms for efficiency and prevention of photo-oxidative stress. In: Roberts JA (ed) Annu Plant Rev Online. Wiley, pp 273–306. https://doi.org/10.1002/9781119312994.apr0666

Roach T, Na CS (2017) LHCSR3 affects de-coupling and re-coupling of LHCII to PSII during state transitions in *Chlamydomonas reinhardtii*. Sci Rep 7:43145. https://doi.org/10.1038/srep43145

Roach T, Na CS, Stöggl W, Krieger-Liszkay A (2020) The non-photochemical quenching protein LHCSR3 prevents oxygen-dependent photoinhibition in *Chlamydomonas reinhardtii*. J Exp Bot 71:2650–2660. https://doi.org/10.1093/jxb/eraa022

Roach T, Böck N, Rittmeier N, Arc E, Kranner I, Holzinger A (2022a) Acquisition of desiccation tolerance in *Haematococcus pluvialis* requires photosynthesis and coincides with lipid and astaxanthin accumulation. Algal Res 64:102699. https://doi.org/10.1016/j.algal.2022a.102699

Roach T, Fambri A, Ballesteros D (2022b) Humidity and light modulate oxygen-induced viability loss in dehydrated *Haematococcus lacustris* cells. Oxygen Basel 2(4):503–517. https://doi.org/10.3390/oxygen2040033

Shimakawa G, Miyake C (2018) Oxidation of P700 ensures robust photosynthesis. Front Plant Sci 9:1617. https://doi.org/10.3389/fpls.2018.01617

Slavov C, Reus M, Holzwarth AR (2013) Two different mechanisms cooperate in the desiccation-induced excited-state quenching in *Parmelia* lichen. J Phys Chem B 117(38):11326–11336. https://doi.org/10.1021/jp402881f

Sonoike K (2025) Photoinhibition and protection of photosystem I. Plant Cell Physiol 66(11):1562–1574. https://doi.org/10.1093/pcp/pcaf079

Stepien P, Johnson GN (2009) Contrasting responses of photosynthesis to salt stress in the glycophyte *Arabidopsis thaliana* and the halophyte *Thellungiella salsuginea*. Plant Physiol 149:1154–1161. https://doi.org/10.1104/pp.108.132407

Vávrová K, Nemcová Y, Pichrtová M (2024) Desiccation and temperature tolerance of green and red *Haematococcus lacustris* (Chlamydomonadales, Chlorophyta) akinetes. Hydrobiologia 851(5):1169–1181. https://doi.org/10.1007/s10750-023-05381-6

Wang J, Sommerfeld M, Hu Q (2009) Occurrence and environmental stress responses of two plastid terminal oxidases in *Haematococcus pluvialis* (Chlorophyceae). Planta 230(1):191–203. https://doi.org/10.1007/s00425-009-0932-4

Watling-Payne AS, Selwyn MJ (1974) Inhibition and uncoupling of photophosphorylation in isolated chloroplasts by organotin, organomercury and diphenyleneiodonium compounds. Biochem J 142(1):65–74. https://doi.org/10.1042/bj1420065

Yamakawa H, Fukushima Y, Itoh S, Heber U (2012) Three different mechanisms of energy dissipation of a desiccation-tolerant moss serve one common purpose: to protect reaction centres against photo-oxidation. J Exp Bot 63(10):3765–3775. https://doi.org/10.1093/jxb/ers062

Zhao J, Yu W, Zhang L, Liu J (2021) Chlororespiration protects the photosynthetic apparatus against photoinhibition by alleviating inhibition of photodamaged-PSII repair in *Haematococcus pluvialis* at the green motile stage. Algal Res 54:102140. https://doi.org/10.1016/j.algal.2020.102140